Application of Mixed Integer Distributed Ant Colony Optimization to the Design of Undamped Single-Tuned Passive Filters based Harmonics Mitigation

Nor H. B. Abdul Kahar[a], Ahmed F. Zobaa[b,*]

[a,b]College of Engineering, Design and Physical Sciences, Brunel University London, Uxbridge, UB8 3PH United Kingdom

[*]Corresponding author: a.zobaa@ieee.org (A.F. Zobaa)

E-mail Address: NorHidayahBinti.AbdulKahar@brunel.ac.uk (N.H.B. Abdul Kahar)

Abstract

The purpose of this study is to find the optimum sizing parameters of the undamped single tuned filter in the nonsinusoidal system by using a new method called Mixed Integer Distributed Ant Colony Optimization. The inductance and capacitance values of the filter are obtained for each criterion where the power factor is maximized, the losses power in Thevenin's resistor is minimized or the transmission efficiency is maximized complying with the technical and practical constraints based on IEEE Std. 519-2014 and IEEE Std. 18-2012. A detailed study has been performed and discussed where global minimum and maximum are achieved after considering the loads being nonlinear, the value of the filter that would introduce resonance, voltage total harmonic distortion, the consequence of the Thevenin's impedance on the load voltage and the practical values of the capacitor. The obtained optimum value of a single tuned filter is used to explain the system performance by evaluating other functions. The effectiveness of the proposed method is proved by comparison with previous publication and other evolutionary computation techniques which are genetic algorithm and particle swarm optimization.

Keywords: Mixed Integer Distributed Ant Colony Optimization, MIDACO, power quality; power system harmonics; passive filters.

1. Introduction

Power system harmonics are the steady-state power quality problem that has existed in the power system since the early development of alternating current system where the distorted waveforms were observed. Recently, nonlinear loads such as rectifiers, power supplies and other devices using solid state switching, have increased, which also increased the concern to the power quality problem [1]. These nonlinear loads produce currents and voltages with a frequency greater than the fundamental frequency, up to a multiple of the fundamental frequency, which is known as the power system harmonics. All of the addressing issues in the power system problem have been very important to pay attention to the power quality problems and the concerns to harmonic distortion problems.

There are several harmonic mitigation techniques to reduce or eliminate the effect of harmonics such as K-factor transformer [2], tuned harmonic filter [3], active filter [4] and shifting transformer [5]. Generally, single tuned filters are the most common passive filters in use due to their simplicity and cost. It has been recommended for nonlinear loads because of its dual purposes of mitigating harmonics and improving power factor. However, the disadvantage of the filter is that it may introduce series or parallel resonance into the system, which needs to be safely away from any significant harmonics [6].

Different approaches optimal filter design for harmonic mitigations have been developed using an Adaptive Carrier Frequency Optimization [7], Non-Dominated Sorting Genetic Algorithm (NSGA-II) [8], Artificial Bee Colony [9], Adaptive Bacterial Foraging Optimization [10], Differential Evolution [11], Cuckoo Search Algorithm [12], Crow Search Algorithm [13] and Bat Algorithm [14].

The first application of Mixed Integer Distributed Ant Colony Optimization (MIDACO) to find the optimal value of single tuned passive filters is presented in this paper taking into consideration the different criteria including different technical and practical constraints using IEEE Std. 519-2014 [15] and IEEE Std. 18-2012 [16]. The proposed method has generally considered the loads being nonlinear, voltage total harmonic distortion, the value of the passive filter that would introduce resonance, the effect of the Thevenin's impedance, and the standard value of capacitor. The major contribution of this methodology is the guarantee of the fast convergence capability to the ideal solution where the results is proved by comparing the results with other effective published techniques which are genetic algorithm (GA) and particle swarm optimization (PSO). Finally, the effectiveness of this proposed technique is demonstrated in examples adopted from IEEE Std. 519-1992.

2. Single-Tuned Passive Filter

A single tuned filter consists of series passive elements, Resistor (R), Inductor (L) and Capacitor (C). Fig. 1 illustrates the filter configuration $R - X$, and $Z - \omega$ plot for single tuned filter.

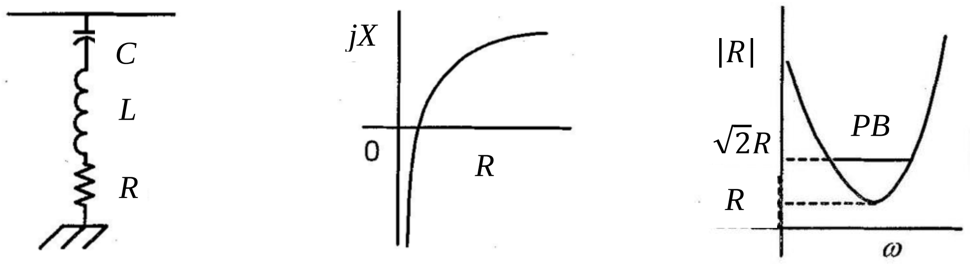

a) Configuration b) R-X Plot c) $Z - \omega$ Plot

Fig. 1. The filter a) configuration, b) $R - X$ Plot and c) $Z - \omega$ Plot for single tuned filter

An ideal single-tuned filter is when the inductor and capacitor of the filter have equivalent reactance and pure resistance at the tuned harmonic. The total filter impedance in Fig. 1(a) is given in Eq. (1) where X_L and X_C in Eq. (2) is inductance and capacitance of the filter, respectively.

$$Z_f = R + j(X_L - X_C) \tag{1}$$

where,

$$X_L = \omega L$$
$$X_C = \frac{1}{\omega C} \tag{2}$$

For single tuned filter, the sharpness of the tuning is determined from the ratio of reactance or capacitance to the resistance at the tuned angular frequency given in Eq. (3) and expressed as

$$f_n = \frac{1}{2\pi\sqrt{LC}} \tag{3}$$

If X_0 is the capacitor's reactance at its tuned frequency

$$X_0 = \omega_n L = \frac{1}{\omega_n C} \tag{4}$$

where the tuned frequency in rad is given by $\omega_n = \sqrt{1/LC}$. Then, substituting Eq. (4) into Eq. (5) gives the value of quality factor *QF*.

$$QF = \frac{X_0}{R} = \frac{1}{R}\sqrt{\frac{L}{C}} \tag{5}$$

In industrial filter design, the typical value of the *QF* is in the range of 20 to 100. The filter that has small *QF* is sharply tuned to lower frequency while high *QF* results in expensive cost of reactor. Therefore, there are standard limitations to limit *QF* for the reactor.

On the other hand, resonant in the power system is the most important effect when adding a single tuned filter in the power system. The series and parallel resonant occur at a frequency below the tuned frequency and expressed as

$$h = \sqrt{\frac{X_C}{X_L}} \tag{6}$$

In theory, maximum efficiency can be achieved if the filter is tuned exactly equivalent to the harmonics that need to be eliminated. However, the filter usually is tuned 3%-10% of the harmonic frequency in Eq. (6) to consider detuning effects. Also, it will provide a margin of safety in case of any changes in temperature or failure with either capacitance or inductance [17].

3. Optimization Problem

3.1 Objective Functions

A single-phase equivalent circuit consists of an undamped single-tuned filter is shown in Fig. 2. It is ideal to gain understanding of the filter by oscillate with minimal damping. Therefore, *LC* filter is obtained by considering no dissipation energy due to resistance by removing of resistor *R* from *RLC* filter.

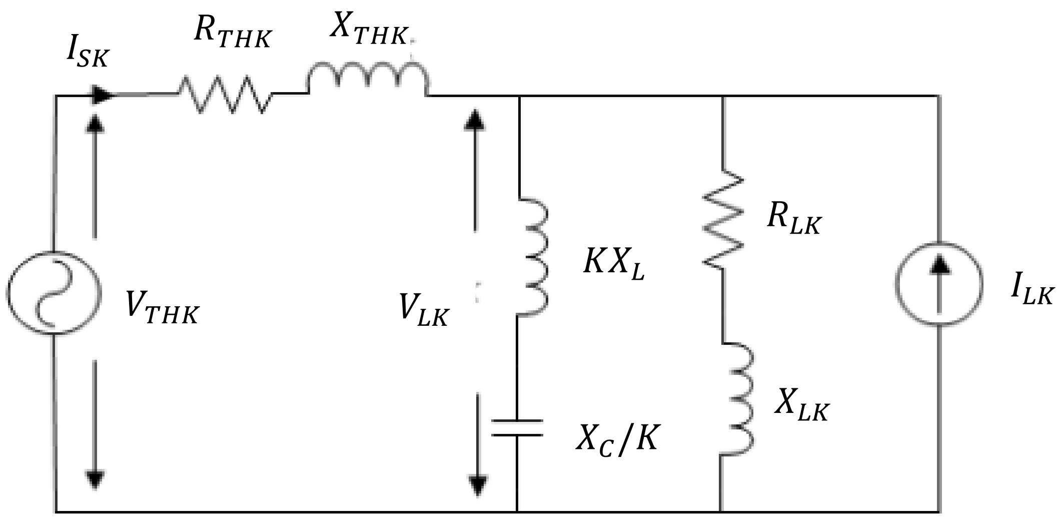

Fig. 2. Single-phase equivalent circuit for *K*th harmonic with undamped single tuned filter

The utility supply is represented using Thevenin's voltage source in Eq. (7) and the nonlinear load is represented by using the harmonic current source in Eq. (8).

$$v_{th}(t) = \sum_{K} v_{thk}(t) \tag{7}$$

and

$$i_{lk}(t) = \sum_{K} i_{lk}(t) \tag{8}$$

where K refers to the present harmonic order.

In the compensated system, the Thevenin's impedance for Kth harmonic is

$$Z_{THK} = R_{THK} + jX_{THK} \tag{9}$$

and the load impedance for the Kth harmonic is

$$Z_{LK} = R_{LK} + jX_{LK} \tag{10}$$

The undamped single tuned filter impedance is denoted by Z_{CK} wherein

$$Z_{CK} = j\left(KX_L - \frac{X_C}{K}\right) \tag{11}$$

To find the load bus impedance Z_{CLK} where Z_{CK} in Eq. (10) is in parallel with Z_{LK} in Eq. (11).

$$Z_{CLK} = \frac{Z_{CK} Z_{LK}}{Z_{CK} + Z_{LK}} \tag{12}$$

So, the total input impedance Z_T is given by substituting Eq. (9) and Eq. (12) into Eq. (13).

$$Z_T = Z_{THK} + Z_{CLK} \tag{13}$$

The equations at each harmonic order K for the compensated source current I_{SK} and the load voltage V_{LK} can be expressed as:

$$I_{SK} = \frac{V_{THK}}{Z_T} + \frac{I_{LK} Z_{CLK}}{Z_T} \tag{14}$$

$$V_{LK} = V_{THK} - I_{SK} Z_{THK} \tag{15}$$

By substituting Eq. (14) and Eq. (15) into Eqs. (16)-(18); the study will include three different criteria of objective functions:

To maximize power factor, PF

$$PF = \frac{P_L}{I_S V_L} = \frac{\sum V_{LK} I_{SK} \cos(\theta_K - \phi_K)}{\sqrt{\sum I_{SK}^2 \sum V_{LK}^2}} \quad (16)$$

To minimize the losses in Thevenin resistor, P_{LOSS}

$$P_{LOSS} = \sum_K I_{SK}^2 R_{THK} \quad (17)$$

To maximize transmission efficiency, η

$$\eta = \frac{P_L}{P_S} = \frac{\sum V_{LK} I_{SK} cos(\theta_K - \phi_K)}{\sum V_{LK} I_{SK} \cos(\theta_K - \phi_K) + \sum I_{SK}^2 R_{THK}} \quad (18)$$

3.2 Constraints

3.2.1 Practical Values of the Capacitor Constraint

The capacitor is chosen from the value of reactive power to the loads wherein this paper considered manufactured values of voltage and reactive power rating of the standard capacitors based on [16]. The capacitor shall be capable to operate without exceeding the following limitation:

a) 135% of RMS value of capacitor current, I_C.

$$I_C = \sqrt{\sum_K I_{CK}^2} \quad (19)$$

where I_{CK} is current of the capacitor at Kth harmonic expressed as

$$I_{CK} = \frac{V_{LK}}{Z_{CLK}} \quad (20)$$

b) 110% of the rated RMS value of the capacitor voltage, V_C.

$$V_C = \sqrt{\sum_K V_{CK}^2} \tag{21}$$

where the voltage of the capacitor at *K*th harmonic, V_{CK} described as

$$V_{CK} = I_{CK} \frac{X_C}{K} \tag{22}$$

c) 120% of rated peak voltage, V_{CP}

$$V_{CP} = \sum_K I_{CK} \frac{X_C}{K} \tag{23}$$

d) 135% of the reactive power of the capacitor, Q_C

$$Q_C = I_C V_C \tag{24}$$

Therefore, all the limitations given in Eqs. (19)-(24) have been considered in this study for reliability and proper operation of the system.

3.2.2 Harmonic Resonance Constraint

In the power system, resonance occurs in series and parallel *RLC* circuit where the inductive reactance of the filter is equivalent to the capacitive reactance.

In series resonance, the circuit has minimum impedance and a small exciting voltage, which results in a high current. Under this condition the power factor is minimum where its high current and very high component voltage values across the inductor and capacitor can cause damage to the circuit. Based on Fig. 2, the series resonance occurs when the load bus impedance, Z_{CLK} in Eq. (12) is connected in series with the Thevenin's impedance, Z_{THK} in Eq. (9) where the resonance series impedance, Z_{SERIES} given in Eq. (25) is equal to the total input impedance Z_T in Eq. (13).

$$Z_{SERIES} = Z_T \tag{25}$$

In contrast, parallel resonance, which occurs in a parallel *RLC* circuit has low admittance and a small exciting current but develops a large voltage. Different with series resonance, the impedance in parallel RLC circuit at resonance becomes maximum wherein the circuit behaves like purely resistive circuit which leading to unity PF.

However, the parallel resonance can increase the harmonic currents and distortion of the voltage in the system. From Fig. 2, inductive supply of Thevenin's impedance and capacitive reactance of the single tuned filter can cause parallel resonance when connected in parallel where the impedance, $Z_{PARALLEL}$ is expressed by substituting Eq. (9) and Eq. (12) into Eq. (26).

$$Z_{PARALLEL} = \frac{Z_{THK} Z_{CLK}}{Z_{THK} + Z_{CLK}} \tag{26}$$

To avoid both series and parallel resonances, the constraint considers the value from Eq. (6) is always greater than harmonic order activating resonance, h_r in Eq. (27) and expressed as

$$h_r = \sqrt{\frac{X_C}{X_L + X_{TH1}}} \tag{27}$$

In addition, the filter also is tuned to slightly lower from Eq. (6) have been considered as a constraint where a tuning frequency is below 3%-10% from the harmonic to be filtered is selected [18].

3.2.3 Additional Constraints

In some utilities, there are surcharges to encourage more efficient use of electricity where these penalties imposed when power factor fall below 90% or 95%, which some even as low as 80%. With the rising cost of energy and anxieties over the efficient delivery of power, achieving acceptable *PF* limits is taken into consideration.

In addition, total harmonic distortions given in Eq. (28) and Eq. (29) is the most common measurements to describe the harmonic content waveform. The total harmonic voltage distortion (*VTHD*) and total harmonic current distortion (*ITHD*) can be expressed as

$$VTHD = \frac{\sum_{K>1} V_{LK}^2}{V_{L1}} \quad (28)$$

$$ITHD = \frac{\sum_{K>1} I_{SK}^2}{I_{S1}} \quad (29)$$

In this paper, Eq. (28) is used as a constraint where the specifying limit is based on [15]. The maximum limit for individual harmonic voltage is 3% and maximum total voltage harmonic distortion is 5% where the objective of the nonlinear loads harmonic current is to control both limitations to not exceed the voltage limits.

4. System under Study

In this study, there are four different cases of industrial plant were simulated where the inductive three-phase load power and reactive power given are 5100kW and 4965kVAR respectively.

Table 1
System parameters and source harmonics under study

Parameters & Harmonics	Case 1	Case 2	Case 3	Case 4
Short Circuit, MVA	150	150	80	80
$R_{TH1}(\Omega)$	0.01154	0.01154	0.02163	0.02163
$X_{TH1}(\Omega)$	0.1154	0.1154	0.2163	0.2163
$R_{L1}(\Omega)$	1.742	1.742	1.742	1.742
$X_{L1}(\Omega)$	1.696	1.696	1.696	1.696
V_{S1}(kV)	2.4	2.4	2.4	2.4
V_{S5}(%)	5	7	5	7
V_{S7}(%)	3	4	3	4
V_{S11}(%)	2	2	2	2
V_{S13}(%)	1	1	1	1
I_{L5}(A)	33	33	33	33
I_{L7}(A)	25	25	25	25
I_{L11}(A)	8	8	8	8
I_{L13}(A)	9	9	9	9

The 60-cycle supply bus voltage is 4.16 kV (line to line) with displacement power factor of 71.65%. The source and load harmonics are randomly selected in all cases. All the data were primarily taken from IEEE Std. 519-1992 publication where all the system parameters and source of harmonics used are described in Table 1.

The different criteria, such as power factor *PF*, losses in Thevenin's resistor P_{LOSS} and transmission efficiency η are expressed as functions of X_C and X_L using Eqs. (16)-(18). After formulating three different criteria of objective functions and constraints involved, the mathematical problem becomes

Maximize $PF(X_C, X_L)$

Minimize $P_{LOSS}(X_C, X_L)$

Maximize $\eta(X_C, X_L)$

Subject to:

- Q_C follows IEEE Std. 18-2012
- $h \leq 0.9 f_n$
- $h > h_r$
- $VTHD \leq 5\%$
- $PF \geq 90\%$ (30)

5. Proposed Optimization Technique

This research proposed MIDACO as an optimization technique where the software implements new extension of Ant Colony Optimization (ACO) in combination with the Oracle Penalty Method.

ACO is one of the meta-heuristics to solve the combinatorial optimization problems was proposed by Marco Dorigo in the early nineties where it was inspired by the foraging behaviour of ant species and the way its function [18]. These ants use pheromone as indirect communications and leave it on the ground to mark the best path to find the food source where it depends on the quality and quantity of the food. The food source should be tracked by other ants by the chemical pheromone trails. ACO exploits a similar mechanism for solving optimization problems.

The new extension of ACO metaheuristics for mixed integer search domains has been developed in MIDACO where the benefit can be seen in its robustness on critical functional properties. The methodology used a concept of pheromone controlled probability functions (PDFs) for discrete domains instead of pheromone table where this method lets an instinctive control of integer variables [19]. In principle, any function that is greater than zero can act as PDF wherein the Gaussian function is the most common one. The advantage of Gaussian Function is that it is easy to implement. However, it also has a disadvantage where it can only focus on one mean. To overcome the problem, Gaussian function, $G^i(x)$ given in Eq. (31) consisting of weighted several alone-dimensional Gaussian Function $g_l^i(x)$ is considered where the equation is described as following:

$$G^i(x) = \sum_{l=1}^{k} w_l^i . g_l^i(x) = \sum_{l=1}^{k} w_l^i \frac{1}{\sigma_l^i \sqrt{2\pi}} e^{-(x-\mu_l^i)^2/2\sigma_l^{i2}} \tag{31}$$

where the function categorized by three triplets w_l^i, σ_l^i and μ_l^i represents the weight for the individual Gaussian functions for the PDF, the standard deviations and means for the corresponding Gaussian functions respectively. The index i is referring to dimension of decision vector and index l is referring to kernel number of the individual Gaussian function.

For constraint handling, MIDACO used new concept of general penalty method called Oracle Penalty Method [20]. This method is based on only one parameter, named Omega (Ω) where it is called 'oracle' because of its predictive nature. In brief, Eq. (32) and Eq. (33) describes the mathematical formulation for extended oracle penalty function.

$$p(x) = \begin{cases} \alpha . |f(x) - \Omega| + (1-\alpha). res(x) & , if \quad f(x) > \Omega \text{ or } res(x) > 0 \\ -|f(x) - \Omega| & , if \quad f(x) \leq \Omega \text{ and } res(x) = 0 \end{cases} \qquad (32)$$

where α is given by

$$\alpha = \begin{cases} \dfrac{|f(x)-\Omega|.\frac{6\sqrt{3}-2}{6\sqrt{3}} - res(x)}{|f(x)-\Omega-res(x)|} & , if \ f(x) > \Omega \text{ and } res(x) < \frac{|f(x)-\Omega|}{3} \\ 1 - \dfrac{1}{2\sqrt{\frac{|f(x)-\Omega|}{res(x)}}} & , if \ f(x) > \Omega \text{ and } \frac{|f(x)-\Omega|}{3} \leq res(x) \leq |f(x)-\Omega| \\ \frac{1}{2}\sqrt{\dfrac{|f(x)-\Omega|}{res(x)}} & , if \ f(x) > \Omega \text{ and } res(x) > |f(x)-\Omega| \\ 0 & , if \ f(x) \leq \Omega \end{cases} \qquad (33)$$

where *res(x)* is a constraint violation

The aim of oracle penalty method is to find global optimal solutions whereas it required running several optimizations to adjust Ω. However, the parameter of Ω only effect to the movement of the shape on the axis which represents the objective function and does not affected the shape of penalty function at all [20].

Based on the black box concept, MIDACO only recognize the returning f(x) and g(x) values for some input variables X. Therefore, a major advantage of the software is where this concept does not require any knowledge of mathematical formulation which gives user a flexibility to define and calculate objective functions and constraints in different form without any restrictions. In addition, the software also is a global optimization algorithm where it does not need to try several initial conditions to ensure that the obtained optimal solution is the global minimum.

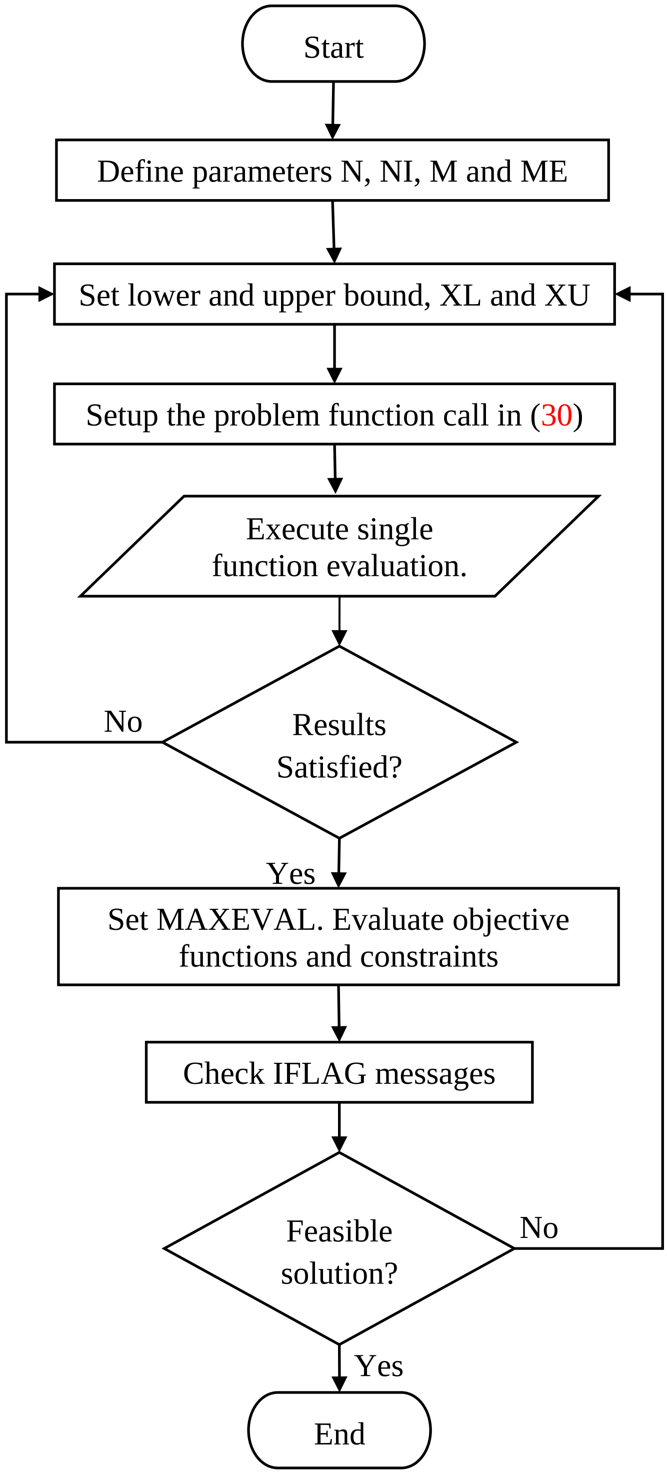

Fig. 3. Flowchart MIDACO

Fig. 3. shows flowchart of the MIDACO where details explanation of the steps to solve the optimization problem are explained as below [21]:

Step 1: Declare the problem dimensions N, NI, M and ME. These refer to the size of F, G and X arrays.

Step 2: Determine the bounds and initial solution X.

Some lower and upper bound must be provided for the decision variables X and the initial point can be any point that lies between XL and XU.

$$\mathrm{XL} \leq \mathrm{X} \leq \mathrm{XU} \text{ (box constraints)}$$

Where vector X contains continuous variables which are stored first and discrete variables are stored last.

Step 3: Setup the problem function call for single tuned filter optimization problem.

a) Input the data of system parameters and source of harmonics.

b) For the input vector of decision variables X, the problem in Eq. (30) is constructing as a function F(X) and G(X) as the form below.

$$\begin{aligned} &\text{Minimize:} && \mathrm{F(X)} \\ &\text{subject to:} && \mathrm{G_i(X)} = 0, \qquad \mathrm{i} = 1,..\mathrm{ME} \\ & && \mathrm{G_i(X)} \geq 0, \qquad \mathrm{i} = \mathrm{ME}+1,..\mathrm{M} \end{aligned}$$

Step 4: Run search algorithm where the initial values of X considers to be X_L and X_C

Step 5: Verifying a problem implementation.

Executes a single function evaluation by setting MAXEVAL=1. This is to manually check if all objective and constraint values reported for the initial values X_L and X_C are reasonable. If 'NO', repeat step 2. Otherwise, continue to the next step.

Step 6: Continue the search algorithm to find optimum solution by setting the MAXEVAL=20000. Once the feasible is reached or the stopping criterion is attained, the algorithm will stop running.

Step 7: Check the IFLAG Messages.

If IFLAG = 1 (feasible solution), continue to the next step. Otherwise, if IFLAG = 2 (infeasible solution) repeat Step 2.

Step 8: The obtained optimum values X_C and X_L are used to define the performance of the system by evaluating some other functions.

Step 9: Save all the outputs file produced by MIDACO.

6. Comparison with Other Published Techniques

In this paper, the proposed technique has been compared with two other evolutionary computation techniques (genetic algorithm and particle swarm optimization) and previous publication [6].

Genetic Algorithm (GA) is a stochastic search technique which based on principles of natural selection and genetics suitable to solve linear and non-linear optimization problems. The main element of GA consists of selection method, crossover method, crossover probability, mutation method, mutation probability and replacement method.where a chromosome represents the solution to the search problem. Another important factor that affects the performance of GA is the population size [22].

Starting with random chromosomes, GA chooses parents to generate a new chromosome from the crossover operation while mutation adds variations. From chromosome, the fitness function is evaluated where the values decide whether the chromosomes are rejected or reserved. As a result, the process may converge to an optimal solution with higher probabilities after a few generations. Because of the probabilistic nature of GA, the process will avoid local minima and tends to the global optimum. However, it did not guarantee finding the optimal solution for the same reason [23].

Particle Swarm Optimization (PSO) was developed by Eberhert and Kennedy where the technique was inspired by bird flocking and fish schooling [24]. PSO is based on a Swarm Intelligence concept where a swarm consists of particles moving in the search space which try to find the possible solution. The term “particles” is referring to the population members where the small mass or volume is subject to the velocities and accelerations in the direction of a better mode of behavior [24].

The PSO algorithm requires adjusting four parameters, maximum value of the velocity, inertia weight, individual and social learning factors [24,25]. In each iteration, each of the particles is updated by two best values before updates its velocity and position. The two best values are the fitness best solution, *Pbest* and best value that is tracked by particle swarm optimizer in the population, *Gbest.* The searching procedures for PSO can be describes based on the equation modified velocity, V_i^{k+i} in Eq. (34) and position updates, X_i^{k+1} in Eq. (35) below.

$$V_i^{k+i} = \omega_0 V_i^k + C_1 rand_1 \times \left(Pbest_i^k - X_i^k\right) + C_2 rand_2 \times \left(Gbest_i^k - X_i^k\right) \quad (34)$$

$$X_i^{k+1} = X_i^k + V_i^{k+i} \quad (35)$$

where ω_0 is an inertia weight typically in the range between 0 to 1. The variable C_1 and C_2 is the cognitive attraction and social attraction, respectively, where the added values for both variables usually in the range $0 < C_1 + C_2 < 4$. These conditions must be satisfied in order to achieve stable equilibrium point of particle swarm. $rand_1$ and

$rand_2$ are two random sequences in the range between 0 to 1. X_i^k is a current position if individual *i* at iteration *k*.

In PSO, no genetic operators like crossover and mutation needed where the particle updates their positions with the modified velocity and PSO also have memory which is important for the algorithm. However, PSO is depending on the initial point and parameters which results in difficulty to find their optimal solution.

In this paper, the proposed technique also has been compared with [6] where the paper used golden section search method. The technique finds the maximum and minimum of objective functions by narrowing the range values where it can be achieved by specifying two conditions given in Eq. (36) and Eq. (37):

$$l_o = l_1 + l_2 \tag{36}$$

$$\frac{l_1}{l_0} = \frac{l_2}{l_1} = R \tag{37}$$

where *R* is golden ratio.

The main advantage of this technique is that it only requires a few steps and function evaluations to locate the optimum solution. However, the algorithm only guarantees the convergence if the objective functions are unimodal.

7. Simulated Results

Four cases compensated systems were simulated where all the results of the system performance were observed and analyzed.

Table 2 summarizes simulated results of the proposed technique for the nonlinear loads using all data in Table 1. The proposed method is implemented by adjusting three parameters which are ants, kernel and oracle (for constraint handling). Thus, the parameter specifications used for controlling the proposed method are ants and kernel which is set to 0 (default). This means that the algorithm will dynamically change the number of ants per generation and maximum kernel number is fixed to 100. Besides, the oracle parameter is set to 0 (default) for handling the constraints.

Table 2
Simulated results of the proposed method

Criteria	X_C (Ω)	X_L (Ω)	*PF* (%)	η (%)	P_{LOSS} (kW)	*VTHD* (%)
Case 1						
Min P_{LOSS}	4.30	0.2058	96.35	99.63	6.12	2.34
Max *PF*	3.95	0.1950	97.18	99.64	6.05	2.35
Max η	4.18	0.2063	96.83	99.64	6.07	2.42
Case 2						
Min P_{LOSS}	4.71	0.2329	93.53	99.61	6.47	3.23
Max *PF*	4.18	0.2053	94.58	99.62	6.37	2.99
Max η	4.43	0.2094	93.63	99.61	6.48	2.88
Case 3						
Min P_{LOSS}	4.87	0.2332	96.31	99.32	11.15	1.90
Max *PF*	4.06	0.1954	98.55	99.35	10.84	1.70
Max η	4.30	0.2002	97.94	99.34	10.91	1.68
Case 4						
Min P_{LOSS}	4.43	0.2082	96.69	99.32	11.16	2.05
Max *PF*	4.43	0.2081	96.69	99.32	11.16	2.05
Max η	4.18	0.1896	97.18	99.33	11.11	1.85

From Table 2, the results show that different optimum solution can be reached for the individual criterion with an extensive improvement of the power factor, reduction of losses in the Thevenin resistor and increase in the transmission efficiency. However, the size of capacitors does not affect the system performance, which means that having large value of capacitor does not mean that the system reaches higher power factor, transmission efficiency or the losses in Thevenin resistor.

For the lower short circuit capacity with same harmonics condition, as Case 1 and 3, it results to a higher power factor. When the Thevenin impedance is high, less harmonic current injected by the harmonic load should flow into the linear compensated load. However, the high value of Thevenin impedance will increase the losses in Thevenin resistor, thus reducing the overall transmission efficiency.

Comparison of the result shows equal short circuit capacity system with an additional supply of voltage harmonics, as Case 3 and 4 will result to the low power factor. This is because the additional harmonics from the increased line current passed through the compensated load. The higher line current cause increase of losses in Thevenin resistor and voltage drop which overall decrease the transmission efficiency.

The results show the objective of the nonlinear loads harmonic current limits is achieved where all the resultants of *VTHD* values for all cases come out well without exceeded the standard limit.

Table 3 shows summary of the simulated results when using GA considering objective functions and constraints in Eq. (30). In order to simulate GA [23], three parameters are assigned in this research as follows: crossover rate, $P_C = 0.8$; mutation probability, $P_m = 0.01$ and population size, $N_P = 50$. The maximum number of iterations is set to 200.

The comparison of the results in Table 2 and 3 shows that the proposed method has outperformed GA where the optimal solution is achieved with better power factor, higher transmission efficiency and lower reduction of losses in Thevenin's resistor for the cases with higher short circuit capacity; refer Case 1 and 2. The results also show that the proposed method might have advantages over increased the losses when compare with the cases with lower short circuit capacity in Case 3 and Case 4. Overall, the results proved that the proposed method has better performance compare to GA where all the resultant values of *VTHD* using proposed method is lower than GA for all cases.

Table 3
Simulated results using genetic algorithm

Criteria	X_C (Ω)	X_L (Ω)	*PF* (%)	η (%)	P_{LOSS} (kW)	*VTHD* (%)
Case 1						
Min P_{LOSS}	4.87	0.2406	95.07	99.62	6.25	2.63
Max *PF*	4.18	0.2062	96.83	99.64	6.07	2.42
Max η	5.41	0.2673	93.49	99.61	6.43	2.77
Case 2						
Min P_{LOSS}	5.22	0.2577	92.25	99.60	6.62	3.23
Max *PF*	4.87	0.2406	93.14	99.61	6.51	2.99
Max η	6.09	0.3008	90.07	99.58	6.90	2.88
Case 3						
Min P_{LOSS}	4.87	0.2406	96.38	99.32	11.14	1.99
Max *PF*	4.18	0.2062	98.36	99.35	10.85	1.80
Max η	4.87	0.2406	96.38	99.32	11.13	1.99
Case 4						
Min P_{LOSS}	5.04	0.2489	95.07	99.30	11.42	2.45
Max *PF*	4.18	0.2062	97.49	99.33	11.05	2.16
Max η	4.71	0.2328	96.06	99.31	11.25	2.34

Table 4 shows summary of the simulated results when using PSO [24]. In order to simulate PSO, some parameters are set as follows: inertia weight, $0.4 \leq C_0 \leq 0.9$; cognitive attraction parameter, $C_1 = 1.0$ and social attraction parameter, $C_2 = 1.0$. In addition, PSO used narrow values of lower and upper bound from $0 \leq X_L \leq 1$ to $0.2 \leq X_L \leq 0.5$ for inductance and from $0 \leq X_C \leq 10$ to $1 \leq X_C \leq 5$ for capacitance to achieve the optimal solution satisfying all different criteria for all cases. The population size is set to 50 and the maximum number of iterations is set to 200.

Table 4
Simulated results using particle swarm optimization

Criteria	X_C (Ω)	X_L (Ω)	PF (%)	η (%)	P_{LOSS} (kW)	$VTHD$ (%)
Case 1						
Min P_{LOSS}	4.18	0.4060	99.19	99.66	5.81	4.30
Max PF	3.95	0.3587	99.28	99.66	5.82	4.09
Max η	5.04	0.2562	94.77	99.62	6.28	2.79
Case 2						
Min P_{LOSS}	4.06	0.4486	99.06	99.65	5.85	5.91
Max PF	3.95	0.3006	98.01	99.65	5.97	4.83
Max η	4.06	0.2418	96.53	99.64	6.13	3.91
Case 3						
Min P_{LOSS}	4.30	0.4310	99.28	99.36	10.70	3.67
Max PF	3.65	0.4098	99.48	99.36	10.88	3.63
Max η	5.22	0.3030	95.64	99.31	11.88	2.59
Case 4						
Min P_{LOSS}	4.30	0.4272	98.97	99.35	10.77	4.69
Max PF	3.74	0.3843	99.33	99.36	10.97	4.48
Max η	4.55	0.2437	94.99	99.30	11.43	2.36

The comparison of the results in Table 4 with Table 2 and 3 shows that different values of bounds results to different values of inductance and capacitance which overall results to different optimal solutions. This proved that PSO is less accurate compare to the other methods since the range values for X_L is far larger than the proposed method and GA when the criteria maximizing power factor and minimizing the losses in Thevenin resistor for all the cases. Besides, the comparison values of *VTHD* also shows that PSO have high values of *VTHD* compare to MIDACO and GA for all cases. Also, the obtained solutions by PSO for Case 2 when the objective function minimizing the Thevenin resistor losses is not satisfy the constraints where the value of *VTHD* is beyond the standard limit.

Table 5 shows the comparison of computation time and number of iterations between the proposed method, GA and PSO.

From Table 5, the results show that the biggest advantage of the proposed method against GA and PSO is the fastest computation time where it can process up to 20 000 number of iterations within 17 to 18 seconds for all cases.

Table 5
Comparison computation time and number of iterations

Criteria	Computation Time, t/s			No. of Iterations		
	MIDACO	GA	PSO	MIDACO	GA	PSO
Case 1						
Min P_{LOSS}	17	33.98	8.31	20 000	4	50
Max PF	17	54.21	7.53	20 000	3	50
Max η	17	67.49	7.12	20 000	6	50
Case 2						
Min P_{LOSS}	18	38.02	8.76	20 000	4	50
Max PF	18	69.27	10.50	20 000	4	50
Max η	18	84.58	9.12	20 000	5	50
Case 3						
Min P_{LOSS}	18	23.94	9.13	20 000	4	50
Max PF	18	43.68	7.92	20 000	5	50
Max η	18	86.17	6.93	20 000	8	50
Case 4						
Min P_{LOSS}	18	35.67	8.51	20 000	4	50
Max PF	17	36.47	7.81	20 000	5	50
Max η	18	119.29	7.34	20 000	8	50

Table 6 presents the statistical measurements for the proposed method, GA and PSO for all cases when the objective function is power factor maximization. Similar results can be obtained for the other objective functions.

It should be mentioned as explained in Section 5: Proposed Optimization Technique, that the proposed optimization algorithm is a global search algorithm that does not need acceptable initial conditions to ensure that the obtained optimal solution is the global minimum or maximum.

Table 6
The statistical tests when criteria maximize *PF*.

Methods	Power Factor, *PF*				
	Min	Max	Mean	Median	Std. Deviation
Case 1					
Proposed Method	93.7303	97.0434	95.2657	95.2146	1.0814
GA	96.9612	97.8850	97.3013	97.0578	0.5078
PSO	98.8990	98.8993	98.8992	98.8992	0.0001
Case 2					
Proposed Method	92.8422	94.8819	94.0731	94.8767	1.0418
GA	96.5421	94.2012	94.5491	94.2021	0.8841
PSO	98.0259	98.0336	98.0311	98.0319	0.0019
Case 3					
Proposed Method	98.0330	98.8572	98.5991	98.7536	0.3380
GA	99.0107	99.0549	99.0200	99.0110	0.0195
PSO	99.4066	99.4146	99.4143	99.4145	0.0013
Case 4					
Proposed Method	96.3780	97.9190	97.7345	97.9128	0.4104
GA	98.0911	98.2382	98.1220	98.0938	0.0650
PSO	98.9253	98.9397	98.9393	98.9397	0.0023

It is clear from Table 6 that the values of standard deviation for the proposed method for all cases are larger compared to GA and PSO which means that the minimum to the maximum optimization values of *PF* is spread apart. This advantage is very important due to the fact that different values should be returned to avoid the resonance occurrence. Also, in this test, we compare the algorithms at their best run where it proved that the proposed method has higher chance to reach global optimal solution before the maximum number of function evaluations is reached. In contrast, it is clear that the variants for GA and PSO are very small and therefore it is difficult to distinguish visually. The better convergence rate of the proposed method during search algorithm is shown in Fig. 4.

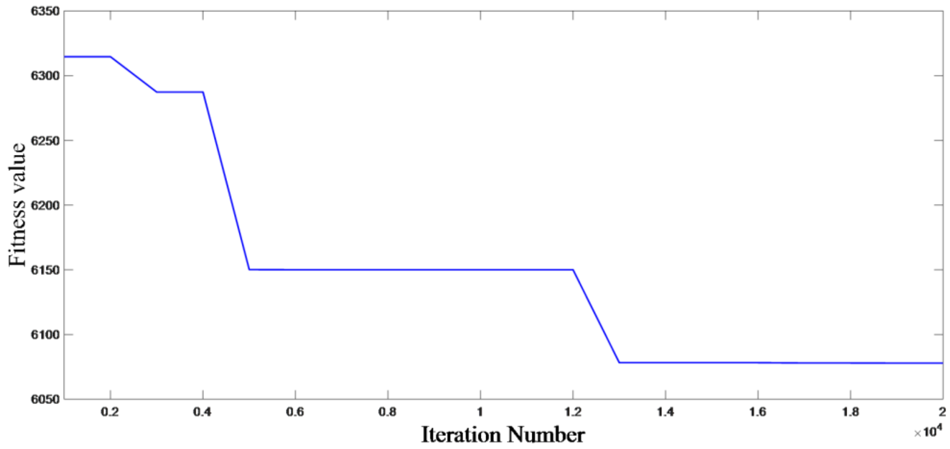

a) Minimize P_{LOSS}

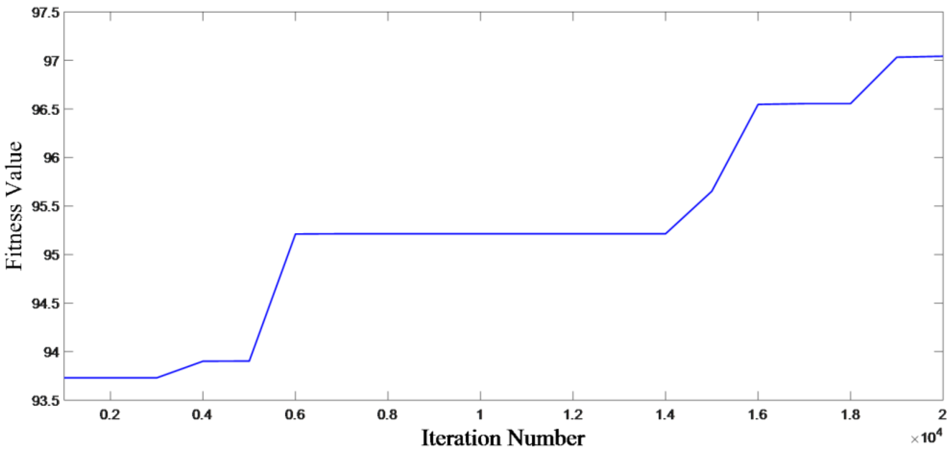

b) Maximize *PF*

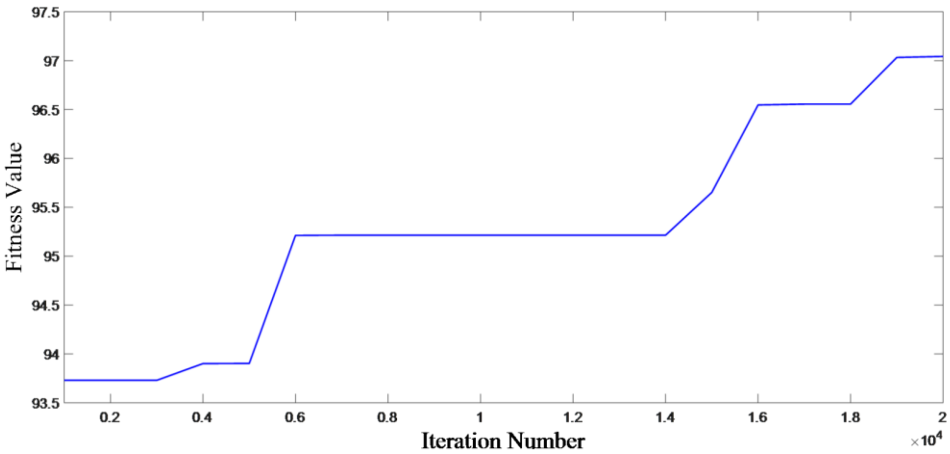

c) Maximize η

Fig. 4. The convergence rate of the MIDACO for case 1

Furthermore, as a figure of merit, the proposed method has fewer control parameters to be adjusted and hence is easier to be implemented compared to GA and PSO. Here it should be noted that adjusting the parameters affect the sensitivity of the results in both GA and PSO.

Since it is important to show how the parameters of the proposed method such as the ants and kernel affect the optimal solution, different cases are studied and presented in Table 7. The kernel parameter must be used in combination with the ants parameter where the 1st setting is the smallest possible, which is useful for CPU-time expensive problems. A relatively low number of ants are considered in the 2nd setting. The 3rd and 4th setting would only be promising for problems, with a fast evaluation time. The 5th setting is the default setting where the results are optimal solution taken from simulated results in Table 2. In addition, it is assumed that all other parameters are kept constant.

From Table 7, the results show lower kernel number will increase the risk of the proposed method getting stuck in a local optimum, while larger kernel number increases the chance of reaching the global optimum. Besides, the results also show that by tuning the parameter of ants might also significantly reduce its performance. Furthermore, it is noticed that near-optimal solutions can be obtained if the parameter specifications used for controlling the proposed method are not well adjusted. Finally, the sensitivity analysis results proved that the base case (Setting 5), achieve better optimal solutions when the number of Kernel is at its maximum and number of ants are dynamically changed at each generation.

Table 7
Effects of changing ants and kernel on the optimal solutions

Setting	Parameters		Power Factor, *PF*			
	Ants	Kernel	Case 1	Case 2	Case 3	Case 4
1	2	2	96.89	92.35	98.57	95.53
2	30	5	94.86	89.87	97.64	94.78
3	500	10	96.22	93.52	88.00	87.46
4	100	50	92.93	91.44	88.81	97.28
5	0	100	97.18	94.58	98.55	96.69

As explained in Section 5: Proposed Optimization Technique, where the parameter of Oracle only effect to the movement of the shape on the axis which represents the objective function and does not affected the shape of penalty function at all [20]. Therefore, Table 8 also has been added to prove that there are no effects to the optimal solutions when changing the values of Oracle. In this test, just oracle parameter is changing while all other parameters are kept constant.

Table 8
Effects of changing oracle on the optimal solutions

Parameters	Power Factor, *PF*			
Oracle	Case 1	Case 2	Case 3	Case 4
1	97.18	94.58	98.55	96.69
3	97.18	94.58	98.55	96.69
6	97.18	94.58	98.55	96.69

Table 9 shows the simulated results to test the effects of changing the number of iterations when criteria maximize *PF*. It proves that the proposed method has higher chance to reach global optimal solution with an increased number of iterations.

Table 9
Simulated results with different number of iterations when criteria maximize the *PF*

Parameters	Power Factor, *PF*			
Number of iterations	Case 1	Case 2	Case 3	Case 4
1000	91.14	89.11	95.99	94.30
10000	93.21	94.58	98.79	96.42
30000	96.57	94.58	98.00	96.88
40000	96.57	94.64	98.06	97.17

Table 10 shows the simulated results for the individual harmonics of the supply current and load voltage.

Table 10
Simulated results for individual harmonics of the supply current and load voltage

Harmonic order, K	Min P_{LOSS}		Max *PF*		Max η	
	I_{SK} (%)	V_{LK} (%)	I_{SK} (%)	V_{LK} (%)	I_{SK} (%)	V_{LK} (%)
Case 1						
5	22.83	1.14	22.50	1.21	22.12	1.27
7	6.67	1.53	6.79	1.50	6.62	1.55
11	2.37	1.17	2.44	1.15	2.37	1.18
13	1.20	0.68	1.22	0.66	1.20	0.68
Case 2						
5	29.63	1.94	31.12	1.74	32.17	1.53
7	8.14	2.16	8.72	2.03	8.70	2.02
11	2.22	1.24	2.38	1.18	2.35	1.19
13	1.16	0.71	1.20	0.68	1.19	0.68
Case 3						
5	13.32	0.79	13.79	0.69	14.01	0.60
7	4.45	1.26	4.72	1.12	4.71	1.12
11	1.66	0.98	1.78	0.88	1.76	0.89
13	0.88	0.68	0.89	0.61	0.89	0.62
Case 4						
5	19.35	0.90	19.35	0.90	20.09	0.68
7	6.10	1.47	6.10	1.47	6.32	1.36
11	1.74	0.92	1.74	0.92	1.80	0.86
13	0.89	0.64	0.89	0.64	0.89	0.60

From Table 10, more harmonic current I_{SK} should be supplied to the compensated load as well as in harmonic voltage V_{LK} when there are additional supply voltage harmonic content for the equal short circuit capacity. These increased the beneficial power gained from the source as the more voltage and current is supplied to the load. However, lower short circuit capacity with same harmonics condition reduced the load power consumption because less harmonic current I_{SK} is supplied to the load as well as harmonic voltage V_{LK}.

Table 11 shows the calculated capacitor limits compared with the standard capacitor limits based on [15].

Table 11
Main capacitor limits based on IEEE Std. 18-2012

Criteria	V_{CP} (%)	V_C (%)	I_C (%)	Q_C (%)
Case 1				
Min P_{LOSS}	68.19	90.34	98.53	86.80
Max *PF*	68.04	90.68	98.20	87.23
Max η	68.09	90.55	98.30	87.05
Standard	120	110	135	135
Case 2				
Min P_{LOSS}	69.85	90.41	102.12	88.04
Max *PF*	69.60	90.64	101.33	88.15
Max η	69.92	90.37	102.35	88.04
Standard	120	110	135	135
Case 3				
Min P_{LOSS}	65.98	88.96	95.21	83.62
Max *PF*	66.15	89.78	95.59	85.02
Max η	66.05	89.36	95.37	84.29
Standard	120	110	135	135
Case 4				
Min P_{LOSS}	67.01	89.32	96.70	84.63
Max *PF*	67.01	89.32	96.71	84.63
Max η	67.02	89.43	96.70	84.80
Standard	120	110	135	135

From Table 11, it shows that the capacitor for all cases is capable to operate without exceeding the standard limit. For the case beyond of the standard limit, it is suggested to practice capacitor with higher voltage rating to avoid the increase in the voltage through the reactor at the fundamental frequency and because of harmonic loading.

Table 12 shows simulated results for the series and parallel harmonic tuning orders when using MIDACO, GA and PSO.

Table 12
Series and parallel harmonic tuning orders

Criteria	MIDACO		GA		PSO	
	h	h_r	h	h_r	h	h_r
Case 1						
Min P_{LOSS}	4.57	3.66	4.50	3.70	3.21	2.83
Max PF	4.50	3.57	4.50	3.60	3.32	2.89
Max η	4.50	3.60	4.50	3.76	4.43	3.68
Case 2						
Min P_{LOSS}	4.50	3.68	4.50	3.74	3.01	2.68
Max PF	4.51	3.61	4.50	3.70	3.62	3.08
Max η	4.60	3.69	4.50	3.83	4.10	3.37
Case 3						
Min P_{LOSS}	4.57	3.29	4.50	3.27	3.16	2.58
Max PF	4.56	3.14	4.50	3.14	2.99	2.42
Max η	4.63	3.21	4.50	3.27	4.15	3.17
Case 4						
Min P_{LOSS}	4.61	3.23	4.50	3.29	3.17	2.58
Max PF	4.61	3.23	4.50	3.14	3.12	2.50
Max η	4.69	3.21	4.50	3.24	4.55	3.31

From Table 12, the results show that the filter is tuned slightly lower from fifth harmonics. This is because it is an advantage to add the filter slightly lower from the harmonic to be filtered to provide sufficient harmonic filtering action. Besides, it also to allow for operation in the bank in case of the removal a few capacitors unit. The results also show the value of harmonic order is always greater than harmonic activating resonance to avoid both series and parallel resonance.

Fig. 5. illustrates the filter, series and parallel impedance in the resonant circuit for individual criteria in case 1.

From Fig. 5, the filter response is evaluated and the characteristic of the filters are described as following:

1) The interaction of Thevenin impedance with the compensated load results in series and parallel resonance.
2) Series impedance, Z_{SERIES} results in series resonance where the impedance reaches the local minimum at the resonant frequency. At resonant point, the inductance and capacitance reactance become the same and cancelling each other, thus making the impedance minimum.
3) Parallel impedance, $Z_{PARALLEL}$ results in parallel resonance where the impedance reaches the local maximum at the resonant frequency, but decreases above or below resonance. There is severe rise in impedance below the tuned frequency because of the proximity of the resonant frequency.
4) For both series and parallel resonant, the impedance is increase with frequency for frequencies above the filter is tuned.
5) If the filter is tuned exactly to the frequency concern, it will result in the sharp increase in impedance where it is enough to coincide with the desired harmonic where the voltage amplification may be disastrous. This also same with series resonance where the current amplification may cause damage in the circuit.
6) Ignoring series or parallel resonance in the analysis would lead to inaccurate results.

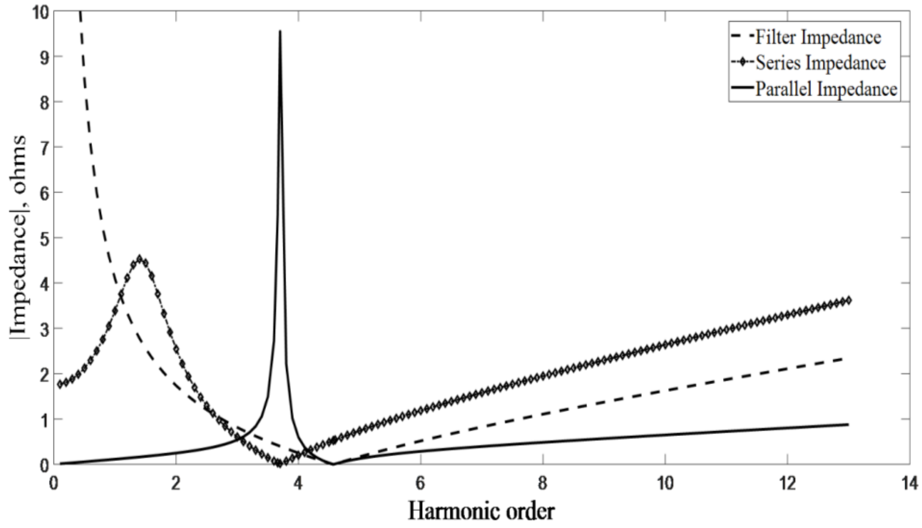

a) Minimize P_{LOSS}

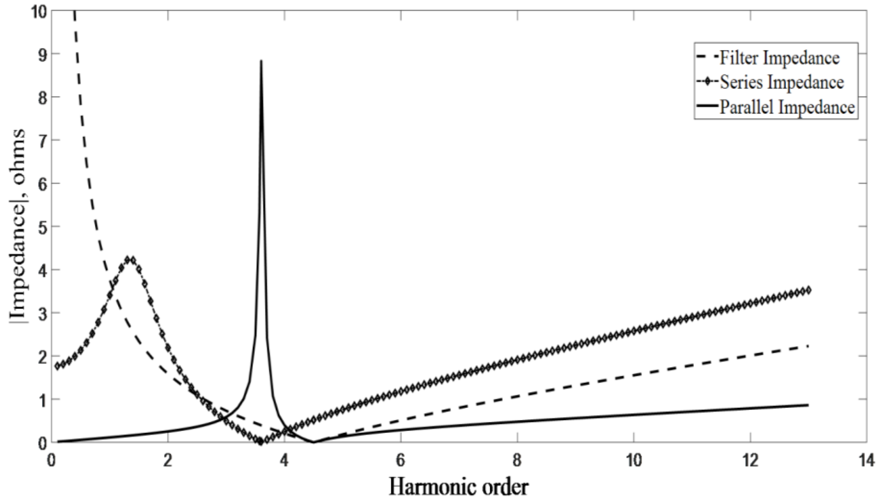

b) Maximize *PF*

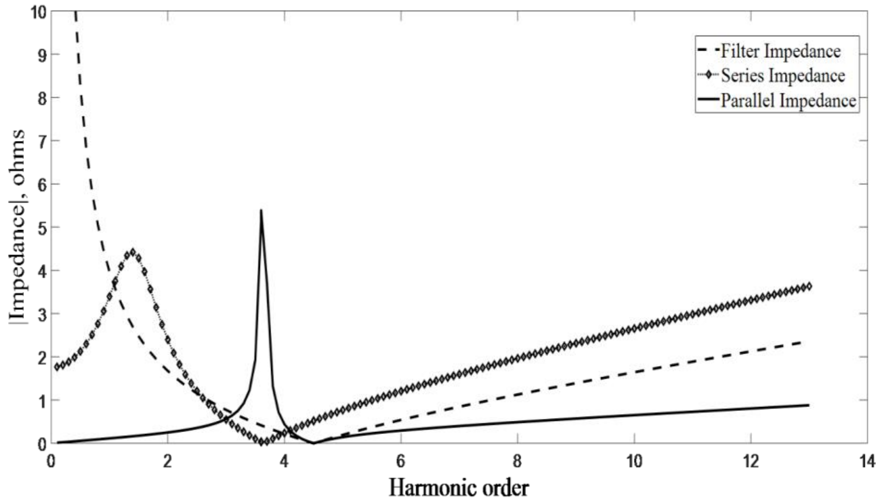

c) Maximize η

Fig. 5. Impedance resonance for case 1

Fig. 6. shows the comparison results of *VTHD* using proposed method with method [6]. The simulation considers the objective functions and constraints in [6] where the mathematical problem addressed in this simulation becomes

Maximize $PF(X_C, X_L)$

Minimize $P_{LOSS}(X_C, X_L)$

Maximize $\eta(X_C, X_L)$

Subject to:

- Q_C follows IEEE Std. 18-1992
- $h > h_r$

After performing calculation of *VTHD* based on the results in [6], the comparison results of *VTHD* show that the proposed method has lower *VTHD* compare to method [6]. From the results, the proposed method gives better accuracy of solution compared to method [6] because all the resultant of *VTHD* values for all cases using method [6] exceeded the standard limit.

In the power system, there is also voltage distortion in the transformer due to the flow of the harmonic currents through transformer's secondary terminal. Therefore, two modifications can be proposed to reduce the voltage distortions, which are transformer impedance and the level of harmonic currents.

Nowadays, low impedance phase shifting transformer has been designed which allows the harmonic currents to be reduced but at the same time providing low impedance. The value of low impedance is very important because it plays a crucial role in reducing the voltage distortion. Besides, the other common method is to reduce the level of harmonic currents by using phase shifting technique.

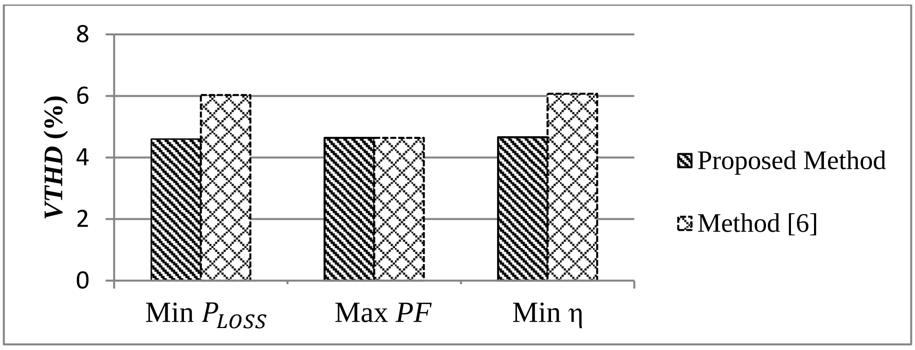

a) Case 1

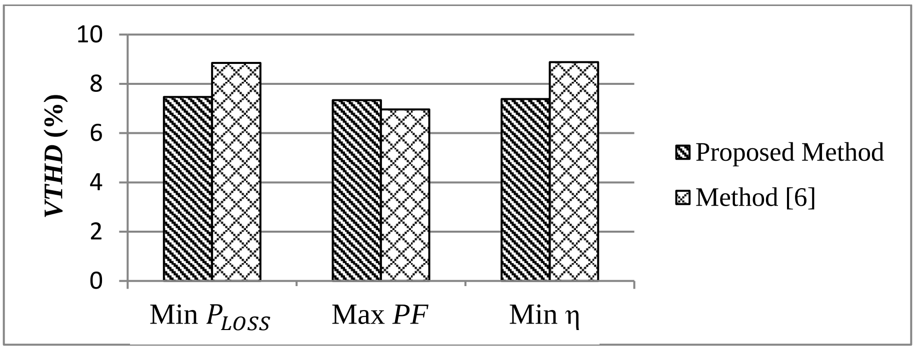

b) Case 2

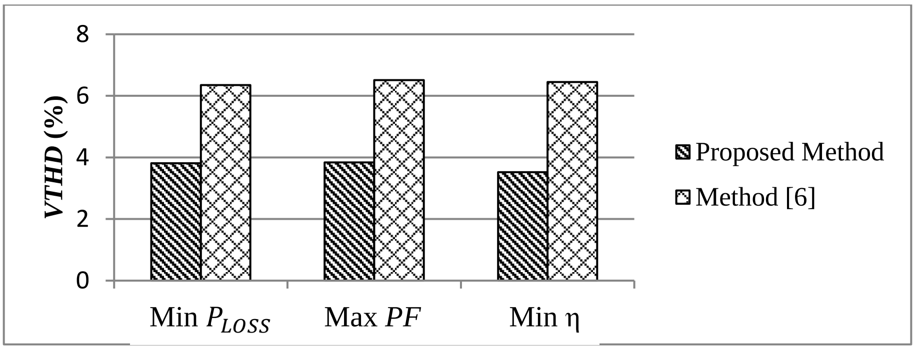

c) Case 3

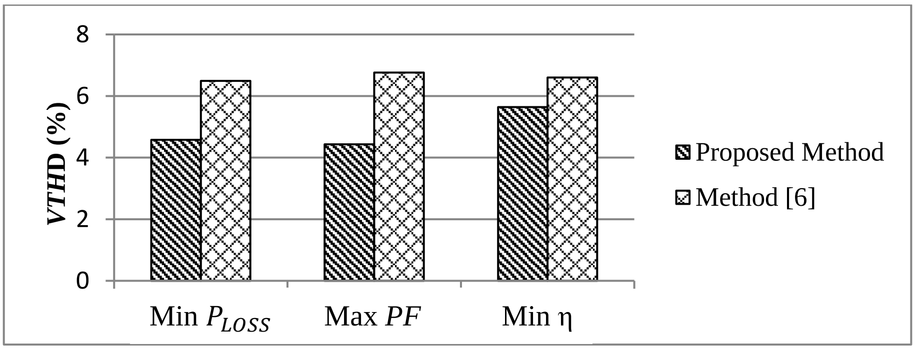

d) Case 4

Fig. 6. Simulated results of *VTHD* based on objective functions and constraints [6].

8. Conclusions

The research raised the important effects with the existence of harmonics of the power quality problem in the power system that consists of nonlinear loads. Consequently, this has increased number of interest in the application of passive filter where single tuned filter which is simple and less expensive has been recommended because of its dual purposes to eliminate harmonics and improving power factor.

In this paper, a mathematical modelling is developed and solved using Mixed Integer Distributed Ant Colony Optimization to optimize the parameters of the single-tuned passive filters having constrained nonlinear problems where the software is inspired by foraging behavior of artificial ants with an extension to mixed integer search domains. The proposed method is compared with the results in other previous publication and two other evolutionary computation techniques which are genetic algorithm and particle swarm optimization. With fewer numbers of control parameters, the proposed method proved its simplicity and fast convergence ability to reach the global solution of the problem.

The filter is designed to achieve the optimal solution satisfying different individual objectives, while considering the loads being nonlinear, the voltage and current distortion at the point of common coupling (PCC), the filter values which would introduce resonance, the effect of the Thevenin's impedance, and the standard capacitor values. The comparative studies validate that the proposed method has outperformed genetic algorithm and particle swarm optimization where all the resultant values of total voltage harmonic distortion using the proposed method are lower than the results obtained by the other methods and the previous publications. The proposed technique denotes a beneficial tool with better accuracy and the effectiveness of the developed algorithm to reach best solution from the certain condition.

Four cases have been tested, where the general performance of the presented method is satisfactory providing different optimum solutions can be reached for the individual criteria with the extensive improvement of the power factor, reduction losses in Thevenin's resistor and increase in transmission efficiency. Finally, the proposed method guaranteed that the proposed filter design has no electrical resonance risks and is capable to operate without exceeding the standard limit for the various performances indices of the system, load and filter.

Nomenclature

R_{LK}, X_{LK}	Load resistance and reactance at harmonic number K (ohms).
R_{THK}, X_{THK}	Thevenin resistance and reactance at harmonic number K (ohms).
X_{TH1}	Thevenin reactance at 1st harmonic order (ohms).
X_L, X_C	Fundamental inductive and capacitive reactances of the filter (ohms)
R	Resistance of the filter (ohms).
V_{THK}	Thevenin voltage at harmonic number K (V).
V_{TH}	RMS value of Thevenin voltage (V).
V_{LK}	Load voltage at harmonic number K (V).
V_{L1}	RMS value of load voltage at fundamental frequency (V).
V_L	RMS value of load voltage (V).
V_{CK}	Capacitor voltage at harmonic number K (V).
V_C	RMS value of capacitor voltage (V).
V_{CP}	Capacitor rated peak voltage (V).
I_{SK}	Source current at harmonic number K (A).
I_{S1}	RMS value of source current at fundamental

	frequency (A).
I_S	RMS value of source current (A).
I_{LK}	Load current at harmonic number K (A).
I_L	RMS value of load harmonic current (A).
I_{CK}	Capacitor current at harmonic number K (A).
I_C	RMS value of capacitor current (A).
P_L	Load power (W).
P_S	Supply power (W).
P_{LOSS}	Losses power in Thevenin resistor (W).
Q_C	Reactive power of capacitor (kVAR).
$VTHD$	Voltage Total Harmonic Distortion (%).
$ITHD$	Current Total Harmonic Distortion (%).
$\theta_{K,}\phi_K$	Angle of load voltage and line current at harmonic number K (rad).
$\omega = 2\pi f$	Angular frequency (rad/s).
N	Number of variables (in total).
NI	Number of integer variables.

M	Number of constraints (in total).
ME	Number of equality constraints.
XL	Lower bound of the search interval.
XU	Upper bound of the search interval.
X	Vector of decision variables.
F(X)	Vector of objective function.
G(X)	Vector of constraint values
MAXEVAL	Maximum number of function evaluation.
IFLAG	Information flag used by MIDACO to indicate final status, warnings or errors.

Conflicts of interest: none

Funding

This research did not receive any specific grant from funding agencies in the public, commercial or not-for-profit sectors

Acknowledgement

The authors would like to thank the anonymous reviewers for their constructive comments and suggestions.

References

[1] S. Rönnberg, M. Bollen, Power quality issues in the electric power system of the future, Electr. J. 29 (2016) 49–61. http://doi.org/10.1016/j.tej.2016.11.006.

[2] P. Bagheri, W. Xu, A technique to mitigate zero-sequence harmonics in power distribution systems, IEEE Trans. Power Deliv. 29 (2014) 215–223. http://doi.org/10.1109/TPWRD.2013.2291866.

[3] A.A.A. El-Ela, S. Allam, H. El-Arwash, An optimal design of single tuned filter in distribution systems, Electr. Power Syst. Res. 78 (2008) 967–974. http://doi.org/10.1016/j.epsr.2007.07.004.

[4] A. Teke, L. Saribulut, M. Tumay, A novel reference signal generation method for power-quality improvement of unified power-quality conditioner, IEEE Trans. Power Deliv. 26 (2011) 2205–2214. http://doi.org/10.1109/TPWRD.2011.2141154.

[5] A. Ghorbani, An adaptive distance protection scheme in the presence of phase shifting transformer, Electr. Power Syst. Res. 129 (2015) 170–177. http://doi.org/10.1016/j.epsr.2015.08.007.

[6] M. Mamdouh, A. Aziz, E.E.A. El-zahab, A.M. Ibrahim, A.F. Zobaa, Power Factor for Nonlinear Loads, 19 (2004) 337–341.

[7] Z. Yang, J. Sun, S. Li, M. Huang, X. Zha, Y. Tang, An Adaptive Carrier Frequency Optimization Method for Harmonic Energy Unbalance Minimization in a Cascaded H-Bridge-Based Active Power Filter, IEEE Trans. Power Electron. 33 (2018) 1024–1037. http://doi.org/10.1109/TPEL.2017.2679028.

[8] J.C. Leite, I.P. Abril, M.E. de L. Tostes, R.C.L. de Oliveira, Multi-objective optimization of passive filters in industrial power systems, Electr. Eng. 99 (2017)

387–395. http://doi.org/10.1007/s00202-016-0420-3.

[9] N.S.P. Singh, N.K. Nair, Artificial bee colony algorithm for inverter complex wave reduction under line-load variations, Trans. Inst. Meas. Control. (2017) 14233121668701. http://doi.org/10.1177/0142331216687019.

[10] M. Mohammadi, A.M. Rozbahani, M. Montazeri, Multi criteria simultaneous planning of passive filters and distributed generation simultaneously in distribution system considering nonlinear loads with adaptive bacterial foraging optimization approach, Int. J. Electr. Power Energy Syst. 79 (2016) 253–262. http://doi.org/10.1016/j.ijepes.2016.01.013.

[11] P.P. Biswas, P.N. Suganthan, G.A.J. Amaratunga, Minimizing harmonic distortion in power system with optimal design of hybrid active power filter using differential evolution, Appl. Soft Comput. 61 (2017) 486–496. http://doi.org/10.1016/j.asoc.2017.08.031.

[12] S. Dhabal, P. Venkateswaran, An efficient gbest-guided Cuckoo Search algorithm for higher order two channel filter bank design, Swarm Evol. Comput. 33 (2017) 68–84. http://doi.org/10.1016/j.swevo.2016.10.003.

[13] S.H.E. Abdel Aleem, A.F. Zobaa, M.E. Balci, Optimal resonance-free third-order high-pass filters based on minimization of the total cost of the filters using Crow Search Algorithm, Electr. Power Syst. Res. 151 (2017) 381–394. http://doi.org/10.1016/j.epsr.2017.06.009.

[14] N.-C. Yang, M.-D. Le, Multi-objective bat algorithm with time-varying inertia weights for optimal design of passive power filters set, IET Gener. Transm. Distrib. 9 (2015) 644–654. http://doi.org/10.1049/iet-gtd.2014.0965.

[15] IEEE Std 519-2014. Recommended Practice and Requirements for Harmonic

Control in Electric Power Systems, IEEE Std 519-2014. 2014 (2014) 1–29. http://doi.org/10.1109/IEEESTD.2014.6826459.

[16] IEEE Standard for Shunt Power Capacitors IEEE Power and Energy Society, 2013.

[17] J.C. Das, Passive Filters - Potentialities and Limitations, IEEE Trans. Ind. Appl. 40 (2004) 232–241. http://doi.org/10.1109/TIA.2003.821666.

[18] M. Dorigo, M. Birattari, T. Stutzle, Ant colony optimization, IEEE Comput. Intell. Mag. 1 (2006) 28–39. http://doi.org/10.1109/MCI.2006.329691.

[19] M. Schlüter, J.A. Egea, J.R. Banga, Extended ant colony optimization for non-convex mixed integer nonlinear programming, Comput. Oper. Res. 36 (2009) 2217–2229. http://doi.org/10.1016/j.cor.2008.08.015.

[20] M. Schlüter, M. Gerdts, The oracle penalty method, J. Glob. Optim. 47 (2010) 293–325. http://doi.org/10.1007/s10898-009-9477-0.

[21] M. Schlüter, M. Gerdts, J.J. Rückmann, A numerical study of MIDACO on 100 MINLP benchmarks, Optimization. 61 (2012) 873–900. http://doi.org/10.1080/02331934.2012.668545.

[22] D.E. Goldberg, Genetic Algorithms in Search, Optimization, and Machine Learning, 1989. http://doi.org/10.1007/s10589-009-9261-6.

[23] A.A. Abou El-Ela, S.M. Allam, M.M. Shatla, Maximal optimal benefits of distributed generation using genetic algorithms, Electr. Power Syst. Res. 80 (2010) 869–877. http://doi.org/10.1016/j.epsr.2009.12.021.

[24] J. Kennedy, R.C. Eberhart, Y. Shi, Swarm Intelligence, 2001. http://doi.org/10.1371/journal.pone.0015505.

[25] M.N. Alam, B. Das, V. Pant, A comparative study of metaheuristic optimization

approaches for directional overcurrent relays coordination, Electr. Power Syst. Res. 128 (2015) 39–52. http://doi.org/10.1016/j.epsr.2015.06.018.